Food Chemistry 398 (2023) 133859

Contents lists available at ScienceDirect

Food Chemistry

journal homepage: www.elsevier.com/locate/foodchem

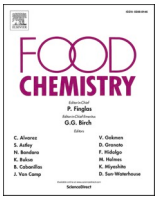

A comprehensive metabolomics analysis of *Torreya grandis* nuts with the effective de-astringent treatment during the postharvest ripening stage

Lili Song [a,b,1], Xuecheng Meng [a,1], Hanbing Song [a], Lingling Gao [a], Yadi Gao [a], Wenchao Chen [a], Weiwei Huan [c], Jinwei Suo [a], Weiwu Yu [a], Yuanyuan Hu [a], Baoru Yang [d], Zuying Zhang [a,b,*], Jiasheng Wu [a,*]

[a] State Key Laboratory of Subtropical Silviculture, Zhejiang A&F University, Lin'an 311300, Zhejiang Province, People's Republic of China
[b] Zhejiang Provincial Key Laboratory of Forest Aromatic Plants-based Healthcare Functions, Zhejiang A&F University, Lin'an 311300, Zhejiang Province, People's Republic of China
[c] Zhejiang Provincial Key Laboratory of Chemical Utilization of Forestry Biomass, College of Chemistry and Materials Engineering, Zhejiang A&F University, Lin'an 311300, Zhejiang Province, People's Republic of China
[d] Food Chemistry and Food Development, Department of Life Technologies, University of Turku, University of Turku, FI-20014 Turku, Finland

ARTICLE INFO

Keywords:
Torreya grandis
Astringent substance
Tannin
$NaHCO_3$ treatment
De-astringency
Metabolome

ABSTRACT

Astringency removal is important for the quality of *Torreya grandis* nut and occurs after harvest. Here, we evaluated the effect of $NaHCO_3$ treatment on astringency removal and compared the differential metabolites of the seed coat and kernel using a UHPLC QQQ-MS-based metabolomics approach. The result revealed the nut astringency was primarily enriched in the seed coat with more soluble tannins. The $NaHCO_3$ treatment greatly shortened the de-astringency process, as indicated by a faster conversion of soluble tannins to insoluble tannins and more acetaldehyde production. Besides, a total of 293 metabolites, including 92 phenolic acids and 37 flavonoids, were tentatively characterized in the seed coat. A further comparative analysis of the metabolomics indicated epigallocatechin, gallocatechin, catechin, procyanidin B1, B2, B3 and C1 to be the major metabolites influenced by the $NaHCO_3$ treatment. This study provides new insights regarding the metabolite differences of *Torreya grandis* nuts processed with different de-astringent treatments.

1. Introduction

Torreya grandis (*T. grandis*) is an evergreen coniferous tree with significant economic and medicinal value in mountainous areas of China. Roasted nuts are popular in China due to their attractive flavor, unique aroma, and multiple healthy bioactive compounds (Suo et al., 2019). Unlike other tree nuts, *T. grandis* nuts need a postharvest ripening process for aromatic synthesis, astringency removal and nutrient conversion (Zhou et al., 2019; Zhang et al., 2020). Although a previous study revealed that appropriate temperature (20 °C) and high relative humidity (90 %) could accelerate the postharvest ripening process (Zhang et al., 2020) and promote aromatic terpene synthesis (Hu et al., 2022), scarce information is currently available regarding the profile and changes in the primary metabolites of *T. grandis* nuts during the postharvest ripening stage.

Astringency, as one of the most important organoleptic properties that determines the quality of *T. grandis* nuts, is generally induced by various phenolic compounds, including tannins that possess a special ability to interact with and precipitate alkaloids, gelatin, and other proteins (Xu et al., 2018). Mild astringency enhances the taste and texture of a number of foods and beverages, most notably tea and red wines (Gu et al., 2004). However, in cases of intensive astringency, the astringent compounds interact with salivary proteins in the mouth and produce a kind of puckering, drying, or rough sensation (Huang & Xu, 2020). According to the solubility in alcoholic solutions, tannins can be divided into soluble and insoluble, and the soluble tannins are the primary source of astringency (Serrano, Puupponen-Pimiä, Dauer, Aura, & Saura-Calixto, 2009). Generally, astringency removal is accompanied by conversion of soluble to insoluble tannins (Pesis, 2005), and with the production of ethanol and acetaldehyde (Taira, Ikeda, & Ohkawa, 2001;

* Corresponding authors at: State Key Laboratory of Subtropical Silviculture, Zhejiang A&F University, Lin'an 311300, Zhejiang Province, People's Republic of China (Z. Zhang).
E-mail addresses: 451882@zafu.edu.cn (Z. Zhang), wujs@zafu.edu.cn (J. Wu).
[1] These authors have contributed equally to this work.

https://doi.org/10.1016/j.foodchem.2022.133859
Received 24 November 2021; Received in revised form 30 July 2022; Accepted 3 August 2022
Available online 6 August 2022

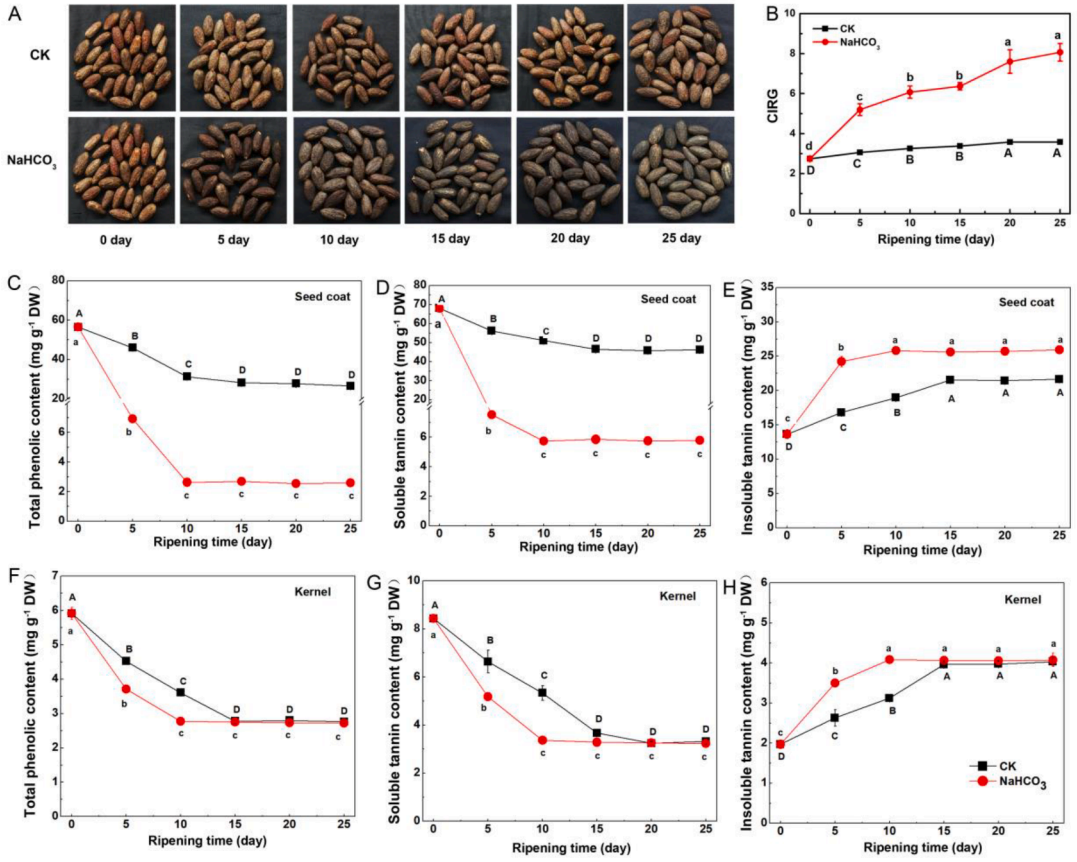

Fig. 1. Changes in the appearance and primary astringent substances in *T. grandis* nuts during the postharvest ripening stage under the control treatment and the $NaHCO_3$ treatment. A, Changes in the seed coat appearance. B, The CIRG value in the seed coat. C, The total phenolic content in the seed coat. D, The soluble tannin content in the seed coat. E, The insoluble tannin content in the seed coat. F, The total phenol content in the kernel. G, The soluble tannin content in the kernel. H, the insoluble tannin content in kernel. The error bars represent the standard error from the three replicates. The different letters indicate the significant differences ($p < 0.05$) during the postharvest ripening stage under the control treatment (uppercase letters) and the $NaHCO_3$ treatment (lowercase letters). DW, dry weight.

Min et al., 2012).

Tannins can also be divided into hydrolyzed tannins and condensed tannins according to their chemical structure (He, Tian, Luo, Qi, & Chen, 2015). Hydrolyzable tannins are compounds that contain a central core of glucose or another polyol esterified with gallic acid or with hexahydroxydiphenic acid (HHDP) In an aqueous solution, HHDP spontaneously dehydrates to their lactone form of ellagic acid (Cos et al., 2003). Condensed tannins do not have a polyol nucleus and are not readily hydrolyzed. They are also known as proanthocyanidins and are oligomeric and polymeric flavan-3-ols that are linked primarily through the C4-C8 or C4-C6 bond (called B-type, dimeric) or doubly linked by an additional ether bond between *C*2-O-C7 (A-type). (+)-Catechin (C), (-)-epicatechin (EC), (-)-epicatechin-3- gallate (ECG), (-)-epigallocatechin (EGC), and (-)-epigallocatechin gallate (EGCG) are considered to be the 5 most common subunits of flavan-3-ols (Dixon, Xie, & Sharma, 2005). Different plant species have different types of dimers, such as procyanidin B1 that is present in grapes and cranberries, B2, present in apples and cocoa beans, B3, present in strawberries and willow catkins, and B4, present in raspberries and blackberries (Haslam, 1977). The perceived astringency is highly correlated with the total tannin concentration, degree of polymerization, subunit composition and distribution (Wei et al., 2020). Unfortunately, studies on astringent substances in *T. grandis* nuts are very limited, and knowledge regarding the changes in astringent substances during postharvest and processing as well as on the mechanism of de-astringency will facilitate the processing to obtain more attractive and healthier products for consumers.

Previous studies found that a 5 % mass fraction of a $NaHCO_3$ treatment had an obvious de-astringent effect on hickory kernels (Fan et al., 2021), while the effect on *T. grandis* nuts remains unclear and the primary metabolites that change during the process requires further identification. Consequently, *T. grandis* nuts were treated with 0.1 M $NaHCO_3$ to profile the metabolomic changes during the postharvest ripening process. The overall objectives of this study are (i) to clarify the effect of $NaHCO_3$ on the de-astringency of *T. grandis* nuts and (ii) to characterize the primary metabolites of *T. grandis* nuts that change under $NaHCO_3$ treatment during the postharvest ripening stage. Our results provide new evidence that shed light on the primary metabolites composition of *T. grandis* nuts with effective de-astringent treatment.

2. Materials and methods

2.1. Plant materials

Cracked *T. grandis* nuts were grown in a commercial orchard in Zhuji, Zhejiang Province, China, and harvested on September 13th, 2020 (approximately 525 days after full bloom). The *T. grandis* nuts with arils were transported to the laboratory within 4 h on the same day of harvest. Next, the arils were removed by hand. Nuts of uniform size with an absence of disease and mechanical wounds were selected for subsequent experiments. The nuts without the arils were left overnight to dissipate the field heat. Before the treatment, the nuts were washed with clean water and then air-dried at 25 °C until there was no excess water on the shell surface. The *T. grandis* nuts were pooled and divided into two lots, each comprised of approximately 30 kg nuts.

Table 1
Effects of different astringency removal treatments on the ethanol and acetaldehyde concentrations in the seed coat and kernel of *T. grandis* nuts.

		Ethanol (μg/g flesh weight)		Acetaldehyde (ng/g flesh weight)	
	Days	CK	$NaHCO_3$	CK	$NaHCO_3$
Seed coat	0	160.02 ± 6.02^{CD}	160.02 ± 6.02^{c}	11.71 ± 1.14^{D}	11.71 ± 1.14^{c}
	5	173.26 ± 3.39^{C}	341.65 ± 8.53^{a}	20.22 ± 2.17^{D}	9.21 ± 1.36^{c}
	10	275.47 ± 6.99^{A}	126.45 ± 3.03^{d}	27.56 ± 5.14^{D}	766.39 ± 36.83^{a}
	15	118.58 ± 6.53^{E}	100.18 ± 8.49^{e}	66.18 ± 13.03^{C}	270.99 ± 8.62^{b}
	20	144.20 ± 4.67^{D}	203.35 ± 11.24^{b}	1315.76 ± 9.77^{A}	24.31 ± 3.32^{c}
	25	216.58 ± 3.34^{B}	184.04 ± 6.83^{b}	98.59 ± 1.58^{B}	17.31 ± 0.07^{c}
Kernel	0	74.94 ± 6.77^{A}	74.94 ± 6.77^{abc}	7.03 ± 0.34^{B}	7.03 ± 0.34^{a}
	5	39.06 ± 6.64^{B}	41.06 ± 2.90^{c}	14.56 ± 0.45^{A}	13.30 ± 1.30^{a}
	10	29.04 ± 0.23^{B}	49.59 ± 6.88^{bc}	5.62 ± 1.02^{B}	8.18 ± 2.52^{a}
	15	42.66 ± 3.55^{B}	61.62 ± 5.21^{bc}	1.41 ± 0.51^{B}	11.24 ± 4.19^{a}
	20	78.49 ± 5.20^{A}	115.81 ± 13.00^{a}	4.47 ± 1.78^{B}	12.78 ± 1.66^{a}
	25	78.49 ± 5.20^{A}	86.68 ± 14.15^{ab}	3.19 ± 1.68^{B}	2.30 ± 0.77^{a}

Note: Errors represent the standard errors from three biological replicates. The different letters indicate the significant differences ($P < 0.05$) during the postharvest ripening stage under the control treatment (uppercase letters) and the $NaHCO_3$ treatment (lowercase letters).

2.2. Postharvest de-astringent treatment

In this experiment, a single-step retting method coupled with conditions of 25 ± 2℃ and a 90 % relative humidity (RH) was adopted according to Ye (2017) and Zhang (2020) with slight modifications, and then different postharvest de-astringency treatments of *T. grandis* nuts were conducted. Approximately 4 kg of *T. grandis* nuts was placed into a sealed storage box (approximately 80 cm in length, 40 cm in width, 15 cm in height), and H_2O treatment (denoted as CK) and $NaHCO_3$ treatment (denoted as $NaHCO_3$) were conducted. CK treatment: The nuts were rinsed with cold water and soaked for 24 h, and then the excess water on the surface was removed. They were placed in a sealed storage frame that was placed in a retort (25 ± 2℃ and 90 % RH). $NaHCO_3$ treatment: The nuts were soaked in 0.1 M $NaHCO_3$ for 24 h, washed with cold water and dried until excess water was removed from the surface; they were then placed in a sealed storage frame that was placed in a retort (25 ± 2℃ and 90 % RH). During the experiment, the pile was turned twice a day. The first sample was collected on day zero after harvest, and then samples were collected at five-day intervals until the 25th day. The seed husks were peeled off, the seed kernels and the seed coats were separated, and they were stored at –80 °C for further analysis. The experiment was performed in three biological replicates for each treatment.

2.3. Chemicals

The anthrone was purchased from the Macklin Biochemical Technology Co., ltd (Shanghai, China). Petroleum ether was purchased from the Sinopharm Co. ltd. (Shanghai, China). Standard compounds such as Coomassie brilliant blue G-250, anhydrous glucose, gallic acid, ethanol, and acetaldehyde were obtained from the Yuanye Company (Shanghai, China). Methanol, acetonitrile and formic acid were HPLC grade and purchased from Merck (Germany). The HPLC and GC standards were purchased from Sigma-Aldrich (St. Louis, MO, USA). Water used throughout the experiment was prepared using the Elix Essential Milli-Q, Milli-Q Reference and TANKPE100 combined purification system (Millipore, Massachusetts, USA).

2.4. Seed coat color determination

Five to six *T. grandis* nuts from the two treatments were randomly selected and then shelled to observe the color of the seed coat at five-day intervals during the treatment. Four points of 90° intervals at the nut equator were measured with a CR-10 colorimeter (KONICA MINOLTA, Inc., Tokyo, Japan), and L* (lightness, 1–100 value range), a* (redness, –60–60 value range), b* (yellowness, –60–60 value range) were recorded accordingly. Next, the a* and b* values were converted into H (hue angle) [H = arc tan (b*/a*)] and C (chroma) ($C = [(a^*)^2 + (b^*)^2]^{0.5}$), which quantified the intensity and purity of the hue. According to the color index of red grapes (CIRG) = (180-H)/(L* + C), the appearance color of the seed coat was reflected (Zhang et al., 2008).

2.5. Determination of the total phenol, soluble and insoluble tannin content

2.5.1. Determination of the total phenol content

The total phenol content was determined according to the method described by Han et al. (2017) with some modifications. (1) Standard curve drawing: 0, 0.25, 0.50, 0.75, 1.00, and 1.25 mL of a 0.2 mg/mL gallic acid solution was added in the colorimetric tube respectively and distilled water was added to 2.0 mL. A total of 1 mL of the Folin-Ciocalteu reagent was then added, and the mixture was mixed well and stored in a dark place for 5 min. Then, 5 mL of 15 % Na_2CO_3 was added, and finally, distilled water was added until the total volume was 10 mL. The solution was mixed well and stored for 1 h. The absorbance was measured at 760 nm and a standard curve was drawn accordingly. (2) Extraction of the sample: Ground dried samples (0.5 g) were extracted using 10 mL methanol for at 25 °C for 2 h. The homogenate was centrifuged at 13,000 *g* for 15 min at 4 °C and the supernatant was used for further measurement. (3) Determination of the sample: A sample of the crude extract (0.5 mL) was added to 1.5 mL of distilled water and 1 mL of the Folin-Ciocalteu reagent. After this, 5 mL of a 15 % Na_2CO_3 solution was added. The mixtures were incubated at 25 °C for 1 h prior to reading at 765 nm. According to the standard curve, the phenol content was calculated according to the following equation.

$$W = \frac{c \times V_T \times K}{m \times V_S}$$

W—The total phenol content of the sample, mg g^{-1} DW;
c—The content of the sample to be tested, mg;
V_T—The total volume of the extract, mL;
m—The quality of the sample, g;
V_s—The sample volume during measurement, mL;
K—Dilution factor.

2.5.2. Determination of the soluble tannin content

Soluble tannins, which are responsible for fruit astringency, were evaluated using the Folin-Denis method described by Arnal and Del Río (2014) with minor modifications. This colorimetric method is based on the reduction of the Folin-Denis reagent by soluble tannins in an alkaline solution. A calibration curve was constructed with tannic acid in the specific concentration range. The ground nuts (1.0 g) were placed in 20 mL of 80 % methanol and the mixture was centrifuged at 5000 *g* for 10 min at 25 °C. The supernatant was then collected and this procedure was repeated twice. Then, the supernatant, containing soluble tannins, was collected from two extractions and was 10-fold diluted with distilled H_2O, and designated as the working solution. For the soluble tannins measurements, 1.0 mL of the working solution and 30 mL of distilled water were mixed, and then 2 mL of the F-D reagent was added and

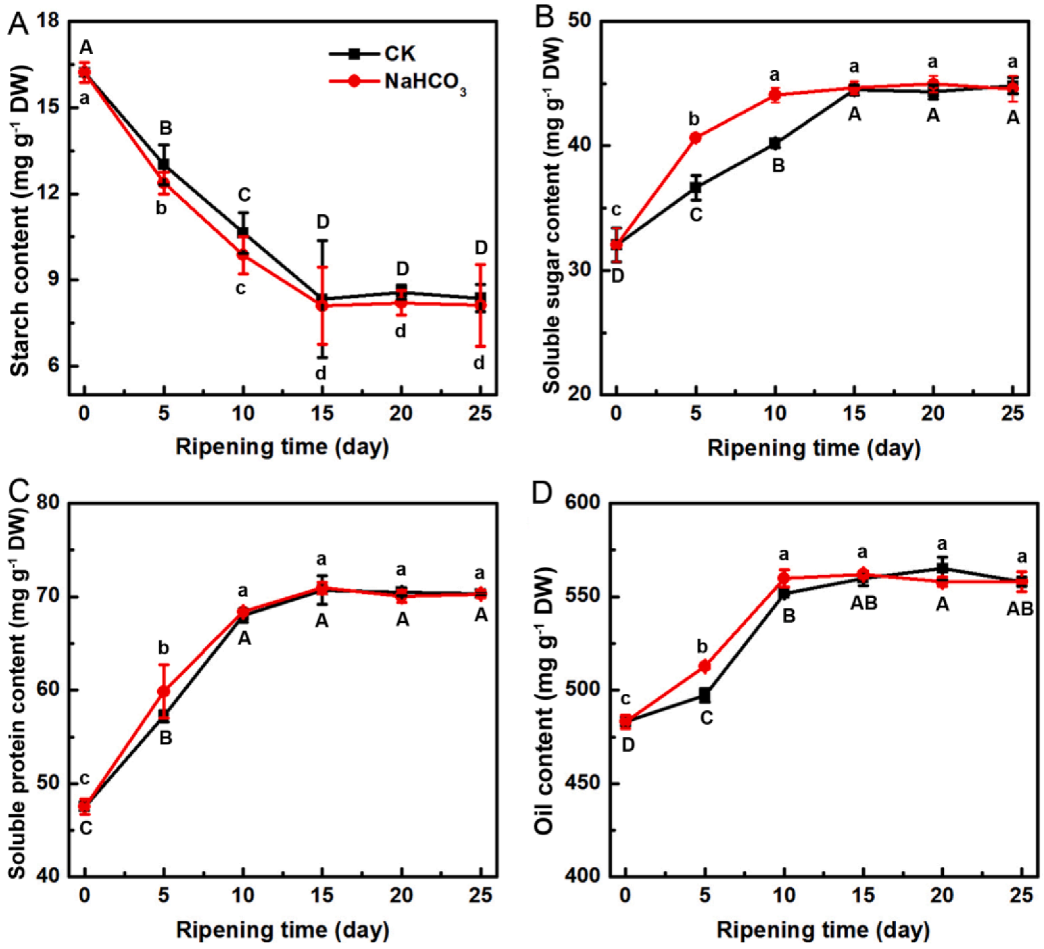

Fig. 2. Content of the starch (A), soluble sugar (B), soluble protein (C), and oil (D) in *T. grandis* nuts during the postharvest ripening stage under the control treatment and the $NaHCO_3$ treatment. The error bars represent the standard error from the three replicates. The various letters indicate the significant differences ($p < 0.05$) during the postharvest ripening stage under the control treatment (uppercase letters) and the $NaHCO_3$ treatment (lowercase letters). DW, dry weight.

mixed well. After 3 min, 10 mL of saturated Na_2CO_3 was added, vortexed, and diluted to 50 mL with distilled water. After the mixture was stored for 2 h at 25 °C, the absorbance was measured at a wavelength of 725 nm. The soluble tannin content was expressed as milligrams of tannic acid per gram of dry weight (mg g^{-1} DW).

2.5.3. Determination of the insoluble tannin content

The insoluble tannins were measured according to the methods reported by Oshida, Yonemori, and Sugiura (1996). After the soluble tannins were extracted, the residue contained insoluble tannins, and then were re-suspended in 5 mL methanol:HCl (99:1, v/v) for 30 min. Next, they were centrifuged at 10,000 g for 10 min at 4 °C. The supernatant was collected and then the procedure was repeated twice. The supernatant was diluted to 50 mL to determine the content of the insoluble tannins (refer to the determination method for soluble tannins).

2.6. Measurement of the ethanol and acetaldehyde concentration

The ethanol and acetaldehyde concentration were measured according to the methods reported by Min et al. (2012). A gas chromatograph (Thermo Scientific™ TRACE 1300™, Thermo Fischer Scientific, Waltham, MA, USA), equipped with a 30 m × 0.25 mm × 0.25 μm capillary column (HP-INNOWAX, Agilent Technologies, Santa Clara, CA, USA) was required. A total of 2 g of the frozen samples were ground with liquid nitrogen and were mixed with 5 mL of a saturated NaCl solution. A total of 3 mL of the mixture was transferred to 10 mL air-tight vials with crimp-top caps. The vials were incubated at 60 °C for 1 h in a water bath and then 0.2 mL of the head-space gas was removed for the gas chromatography. The injector, detector and oven temperatures were set at 150, 160 and 100 °C, respectively. *sec*-butyl alcohol was added to each vial as an internal control. The results were calculated using standard curves for ethanol and acetaldehyde, respectively.

2.7. Measurement of the oil, starch, soluble sugar and soluble protein content

The oil content was measured according to the methods reported by Zhang (2020). The oil was extracted from the nuts with a petroleum ether solvent at a boiling point range of 30–60 °C in a Soxhlet device for 8–12 h. After defatting, the samples were dried overnight (10–12 h) in a fume hood to remove the residual petroleum ether and weighed to calculate the lipid content.

Oil content = (dry weight before defatting – dry weight after defatting)/dry weight before defatting

Next, the residue was used for the determinations of the starch, soluble sugar and soluble protein. Both the content of soluble sugar and starch were determined using anthrone colorimetry (Li & Li, 2013). The residue (without soluble sugar) was added to 10 mL of distilled water and then boiled for 15 min. After cooling, 20 mL of perchloric acid was added, and the solution was left for 15 min at 25 °C. After centrifugation (10,000 *g*, 15 min), the supernatant was collected. This extraction procedure was performed three times, and the supernatant was collected

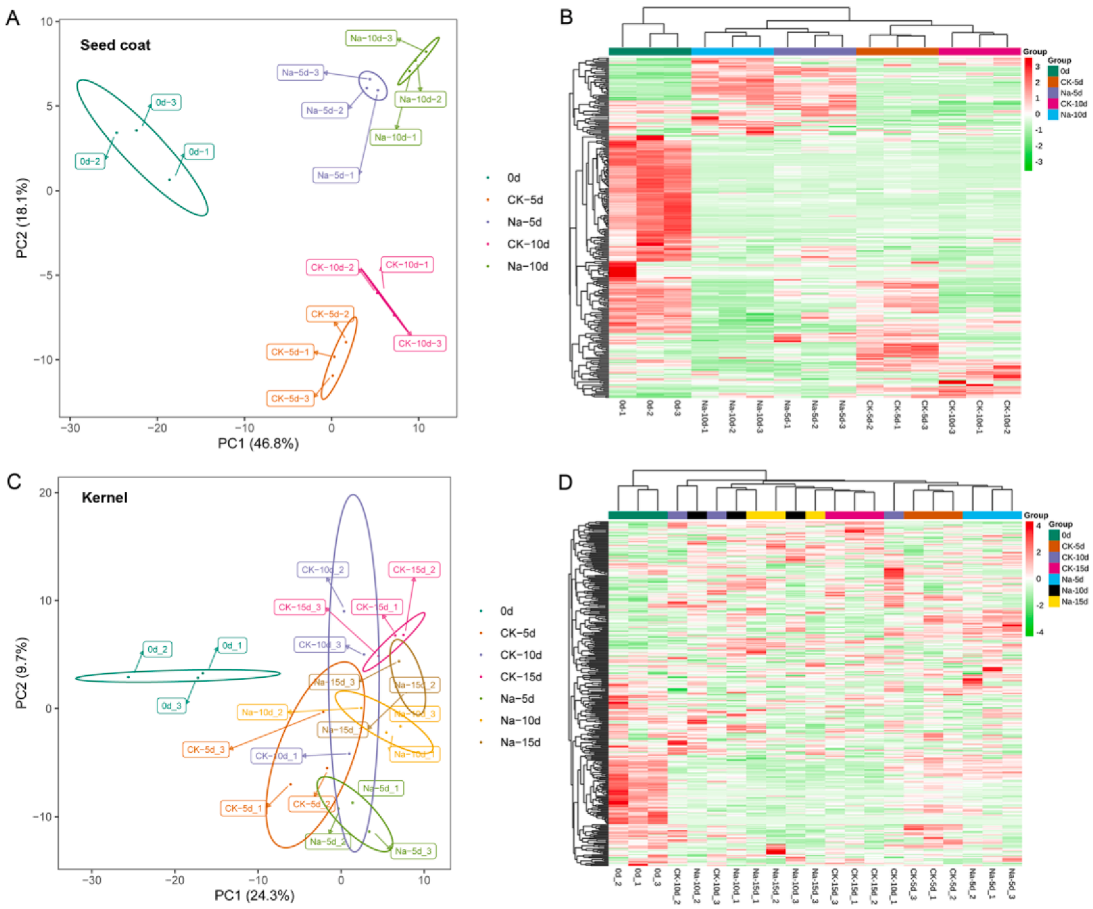

Fig. 3. Principal component analysis (PCA) of the metabolites in the seed coat (A) and kernel (C) and the heatmap analysis in the seed coat (B) and kernel (D) of *T. grandis* nuts during the postharvest ripening stage under the control treatment and the $NaHCO_3$ treatment. Note: 0 d, day 0 of the seed coat or kernel; CK-5d, day 5 of the control seed coat or kernel; CK-10d, day 10 of the control seed coat or kernel; Na-5d, day 5 of the $NaHCO_3$ treated seed coat or kernel; Na-10d, day 10 of the $NaHCO_3$ treated seed coat or kernel; Na-15d, day 15 of the $NaHCO_3$ treated kernel.

into a 100 mL volumetric flask. Next, 1 mL of the solution and 5 mL of the anthrone reagent were mixed and placed in a boiling water bath for 10 min. After being cooled, they were placed in the dark for 10 min to measure the absorbance at 620 nm for the starch content analysis. The soluble protein content was determined with reference to the Coomassie Brilliant Blue G-250 method and measured at 595 nm (Read & Northcote, 1981). The starch, soluble sugar, soluble protein and oil contents are shown as g kg^{-1} dry weight.

2.8. Widely targeted metabolomics analysis

2.8.1. Sample preparation and extraction

The $NaHCO_3$-treated nuts and relevant control nuts, including the seed coats on Day 0, Day 5, and Day 10 and kernels on Day 0, Day 5, Day 10, and Day 15, were processed for a further metabolomic analysis. The samples were placed in a freeze dryer (Scientz-100F) for vacuum freeze drying and then ground into powder in a grinder (MM 400, Retsch, Germany). Approximately 100 mg of ground nuts was dissolved in 1.2 mL of 70 % methanol extract and vortexed once every 30 min for 30 s. Each was vortexed six times in total, and the samples were placed in a refrigerator overnight at 4 °C. After centrifugation (11,000 *g*, 10 min), the supernatant *was* filtered through a 0.22 μm PTFE Millipore membrane for ultra-performance liquid chromatography (UPLC) (SHIMADZU Nexera X2) and a tandem mass spectrometry (MS/MS) (Applied Biosystems 4500 QTRAP) analysis using an SB-C18 analytical column (2.1 × 100 mm, 1.8 μm, Agilent Technologies, Foster City, CA).

2.8.2. UPLC conditions

The analytical conditions were as follows: solvent A (formic acid: ultrapure water, 1: 1000, v/v) and *solvent* B (formic acid: acetonitrile, 1: 1000, v/v). The gradient programme was a 5 % B phase ratio at 0 min, the B phase linearly increased to 95 % within 9.0 min and was maintained at 95 % for 1.0 min, and this was followed by a decrease to 5 % from 10.0 to 11.1 min and remained constant until 14.0 min. The flow rate was 0.35 mL min^{-1} at 40 °C, the injection volume was 4 μL. The effluent was then connected to an ESI-triple quadrupole-linear ion trap (QQQ-LIT) mass spectrometer.

2.8.3. ESI-Q TRAP-MS/Ms

Linear ion trap (LIT) and triple quadrupole (QQQ) scans were performed on a triple quadrupole-linear ion trap mass spectrometer (Q TRAP) and an API 4500 Q TRAP LC/MS/MS system equipped with an ESI Turbo Ion-Spray interface operating in positive and negative ionization modes and controlled by Analyst 1.6.3 software (AB Sciex). The ESI source operation parameters were as follows: ion source, turbo spray; ion source temperature, 550 °C; positive ion spray (IS) voltage, 5,500 V; negative IS voltage, −4,500 V; the ion source gas I (GSI), gas II (GSII), curtain gas (CUR) were set at 55, 60, and 25.0 psi, respectively; and the collision-induced ionization (CAD) parameter was high. Instrument tuning and mass calibration were performed using 10 and 100 μmol/L polypropylene glycol solutions in the QQQ and LIT modes, respectively. The QQQ scans were acquired as multiple reaction monitoring (MRM) mode experiments with the collision gas (nitrogen) set to medium. The de-clustering potential (DP) and collision energy (CE) for the individual MRM transition were performed with further DP and CE

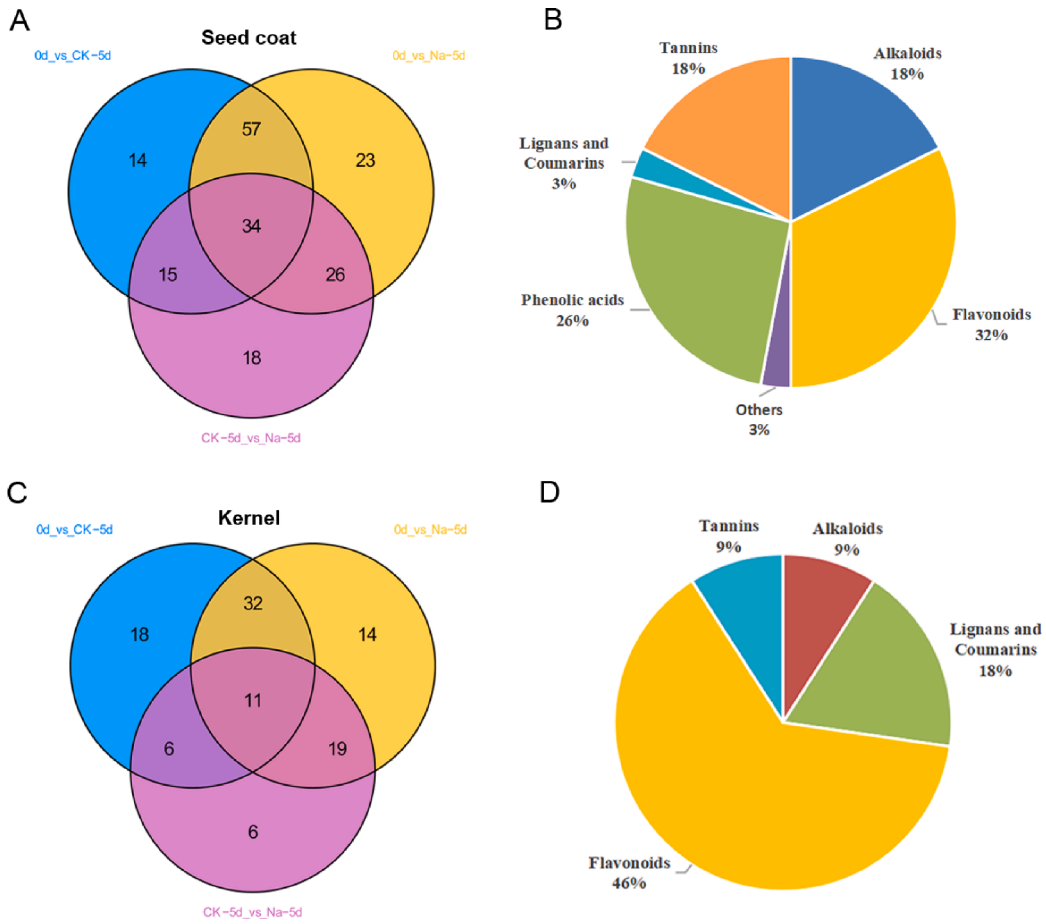

Fig. 4. Venn diagram analysis of the metabolites in the seed coat (A) and kernel (C) and the metabolite composition analysis in the seed coat (B) and kernel (D) of *T. grandis* nuts during the postharvest ripening stage under the control treatment and the $NaHCO_3$ treatment.

optimization. A specific set of MRM transitions were monitored for each period based on the metabolites eluted within this period.

2.8.4. Qualitative and quantitative analysis of the metabolites

High-resolution mass spectrometry AB sciex 6600 QTOF for qualitative detection of mixed samples was employed in this study which indeed provided exact mass of compounds for identification purposes and formula prediction. A qualitative analysis of the metabolites was conducted by a comparison of the accurate precursor ion (Q1), the product ion (Q3) values, the retention time (RT), and the fragmentation pattern based on the self-built metware database (MWDB) (Wuhan Metware Biotechnology Co., ltd., Wuhan, China) (Chen et al., 2013) and the public metabolite database. To ensure the accuracy of the metabolite annotations, the repeated signals of K^+, Na^+, $NH4^+$, and other large molecular weight substances were eliminated during identification.

Then AB sciex4500 Q TRAP for relative quantification of samples was used owing to its higher senstivity, combining the advantages of non-targeted and targeted metabolomics. A quantitative analysis of the metabolites was employed with the MRM mode of the QQQ MS. The precursor ions (parent ions) of the target substances were screened, and the ions corresponding to other molecular weight substances were excluded to initially eliminate interference. The precursor ions were fragmented after induced ionization by collision for the production of fragment ions that were then filtered using a QQQ for the selection of the characteristic fragment ions and elimination of interference from non-target ions, making the quantification more accurate and repeatable. The mass spectrum peak of each metabolite in each sample was corrected according to the RT and the peak shape of each metabolite. The corresponding relative metabolite contents were represented as chromatographic peak area integrals (Hu, Wang, Hu, & Xie, 2020). A parameter called the variable importance in projection (VIP) was used to examine the relative importance of each metabolite in the PLS-DA model. Metabolites with VIP ≥ 1 and fold change ≥ 2 or fold change ≤ 0.5 were considered differential metabolites for the group discrimination (Yang et al., 2019).

2.9. Statistical analyses

The figures were created with Origin 8.0 (MicroCal Software). The data are presented as the mean $\pm$ standard deviation (SD). The significant differences were determined using SPSS Statistics 20.0 (SPSS Inc., Chicago, IL, USA). In addition, a principal component analysis (PCA) was used to comprehensively evaluate the impact of the $NaHCO_3$ postharvest treatments on the de-astringency of *T. grandis* nuts.

3. Results and discussion

3.1. Effect of the $NaHCO_3$ treatment on the astringency removal of T. grandis nuts

In practice, the ripening process of *T. grandis* nuts is considered to be complete when the interior seed coat turns completely dark black. The color of the interior seed coat of *T. grandis* nuts on Day 0 was reddish and gradually turned black on Day 5 under the $NaHCO_3$ treatment, whereas it showed only a slight change under the CK treatment (Fig. 1A). The CIRG value change was consistent with the color change (Fig. 1B). It has been reported that the color change in the seed coat may be caused by a change in the phenolic substances after oxidization (Chazarra, Garcia-

Table 2
A list of common differentially down-regulated metabolites identified on Day 5 under the control treatment and $NaHCO_3$ treatment of *T. grandis* nuts.

Sample	Compounds	Class I	CK-5d-1	CK-5d-2	CK-5d-3	Na-5d-1	Na-5d-2	Na-5d-3	Fold_Change (CK-5d_vs_Na-5d)	Type (CK-5d_vs_Na-5d)	Identification method
Seed coat	Epigallocatechin	Flavonoids	4.05E + 05	3.68E + 05	4.14E + 05	2.10E + 05	9.46E + 04	1.58E + 05	0.389797071	down	Standard
	Gallocatechin	Flavonoids	1.72E + 06	1.43E + 06	1.71E + 06	9.32E + 05	5.09E + 05	6.69E + 05	0.433277894	down	Standard
	Nepetin (5,7,3′,4′-Tetrahydroxy-6-methoxyflavone)	Flavonoids	3.38E + 05	1.98E + 05	3.22E + 05	6.95E + 04	3.80E + 04	5.50E + 04	0.189518245	down	Manual identification
	Protocatechuic acid-4-O-glucoside	Phenolic acids	6.56E + 04	2.97E + 04	5.65E + 04	9.00E + 00	9.00E + 00	9.00E + 00	0.000177841	down	Manual identification
	3,4,5-Trimethoxyphenyl-1-O-Glucoside	Phenolic acids	1.45E + 05	2.58E + 05	2.10E + 05	9.00E + 00	9.00E + 00	9.00E + 00	4.40299E-05	down	Manual identification
	6-O-Caffeoyl-D-glucose	Phenolic acids	1.80E + 05	9.60E + 04	1.64E + 05	6.35E + 04	4.56E + 04	1.34E + 04	0.278255357	down	Manual identification
	Syringetin	Flavonoids	2.27E + 04	1.53E + 04	3.98E + 04	1.92E + 03	9.00E + 00	9.00E + 00	0.024953359	down	Standard
	Procyanidin B2	Tannins	1.59E + 05	1.02E + 05	1.43E + 05	7.20E + 04	5.58E + 04	4.64E + 04	0.430495069	down	Standard
	Procyanidin B3	Tannins	3.14E + 05	1.91E + 05	1.54E + 05	9.88E + 04	3.78E + 04	6.10E + 04	0.300302353	down	Standard
	Procyanidin B1	Tannins	4.85E + 04	4.43E + 04	3.97E + 04	2.68E + 04	1.19E + 04	2.09E + 04	0.450080388	down	Standard
	Procyanidin C1	Tannins	9.19E + 03	3.44E + 03	8.50E + 03	9.00E + 00	9.00E + 00	9.00E + 00	0.001277556	down	Manual identification
Kernel	Catechin	Flavonoids	1.40E + 04	1.17E + 04	6.55E + 03	2.78E + 03	7.89E + 03	4.75E + 03	0.477744826	down	Standard
	Gallocatechin	Flavonoids	8.04E + 03	7.78E + 03	1.28E + 04	2.67E + 03	1.75E + 03	2.78E + 03	0.251614256	down	Standard
	Isorhamnetin-7-O-glucoside (Brassicin)	Flavonoids	1.88E + 04	1.50E + 04	3.07E + 04	1.13E + 04	5.17E + 03	9.23E + 03	0.39742581	down	Manual identification
	Myricetin-3-O-galactoside	Flavonoids	2.07E + 04	1.46E + 04	1.80E + 04	9.00E + 00	9.00E + 00	9.00E + 00	0.000506671	down	Manual identification
	Myricetin-3-O-glucoside	Flavonoids	1.68E + 04	9.81E + 03	1.67E + 04	9.00E + 00	9.00E + 00	9.00E + 00	0.000622988	down	Manual identification
	Limocitrin-3-O-galactoside	Flavonoids	4.83E + 04	2.96E + 04	4.87E + 04	2.60E + 04	1.90E + 04	1.33E + 04	0.460177411	down	Manual identification
	Syringetin-7-O-glucoside	Flavonoids	1.46E + 04	1.12E + 04	8.54E + 03	5.08E + 03	8.39E + 03	3.69E + 03	0.499012746	down	Manual identification
	Procyanidin B3	Tannins	9.55E + 03	9.00E + 00	1.00E + 04	9.00E + 00	9.00E + 00	9.00E + 00	0.001377045	down	Standard

Note: The main astringent substances are denoted in RED. Metabolites with VIP $\geq$ 1 and fold change $\leq$ 0.5 were considered differential metabolites for group discrimination. Standard: the metabolite was confirmed by chemical standards. Manual identification: the metabolite was confirmed by comparison of the accurate precursor ion (Q1), product ion (Q3) values, the retention time (RT), and fragmentation pattern based on the metabolite database.

Carmona, & Cabanes, 2001). Indeed, the total phenol content in the seed coat of the two de-astringent treatments displayed a decreasing trend, and the nuts treated with $NaHCO_3$ showed a more pronounced decreasing trend compared to those under the CK treatment, from 56.47 mg g^{-1} on Day 0 to 2.63 mg g^{-1} on Day 10 (Fig. 1C).

Typically, tannins are the primary phenolic astringency compounds that can interact and precipitate alkaloids, gelatin, and other proteins (Xu et al., 2018). The content of soluble tannins has generally been considered as the primary influence on perception of astringency that disappears below a threshold of 0.1 % (Soares et al., 2020). Studies have reported that the removal of astringency is reflected in a dramatic decrease of the soluble tannin content and a corresponding increase in the insoluble tannin content (Min et al., 2012). In the present study, both the CK and $NaHCO_3$ treatments prompted de-astringency in the seed coat manifested as a dramatic decrease in the soluble tannin concentration, with $NaHCO_3$ treatment decreasing three times as much as the control (Fig. 1D). The opposite trend was observed in the insoluble tannin content of the seed coat under the two de-astringent treatments that showed an upward trend (Fig. 1E). The changing trends in the total phenols, soluble tannin, and insoluble tannin in the kernels under the two de-astringent treatments were similar to those of the seed coats, and the soluble tannin contents in the seed coats were significantly higher than the levels found in the kernels (Fig. 1), indicating that the nut astringency was primarily in the seed coat rather than the kernel.

Ethanol and acetaldehyde are the primary products in anaerobic fermentation, and acetaldehyde is the primary compound that interacts with the soluble tannins to render them insoluble (Taira et al., 2001; Min et al., 2012). The contents of ethanol and acetaldehyde were significantly higher in the seed coat than in the kernel (Table 1), indicating that de-astringency primarily occurred in the seed coat. The overall trend of changes in the ethanol and acetaldehyde contents were analyzed, and the peaks of the ethanol and acetaldehyde contents in the $NaHCO_3$ treated nuts were significantly earlier than those in the control. For example, the ethanol content of the $NaHCO_3$ treated seed coat reached a peak value of 341.65 ug g^{-1} on the 5th day, while the control reached a peak of 173.26 ug g^{-1} on the 10th day, and its maximum peak value was obviously lower than that of the $NaHCO_3$ treated seed coat (Table 1). In terms of the acetaldehyde content, the seed coat under the $NaHCO_3$ treatment showed a significantly higher acetaldehyde content compared with the samples under the CK treatment from Day 5 to Day 15. However, the seed coat under the CK treatment showed a significantly higher acetaldehyde content than under the $NaHCO_3$ treatment from Day 15 to Day 25, indicating the maximum peak value of acetaldehyde in the $NaHCO_3$ treated nuts was obviously earlier than those in the control. The content of acetaldehyde in the persimmon fruit increased under the postharvest ethylene and CO_2 treatment, indicating

that the process of de-astringency was accelerated accordingly (Yin et al., 2012). Therefore, the results showed that the $NaHCO_3$ treatment effectively removed astringency and accelerated the process of de-astringency in *T. grandis* nuts, which was consistent with the change trend of the tannin content (Fig. 1).

3.2. The $NaHCO_3$ treatment maintained the nutritional quality of the *T. grandis* nuts

The starch in the seeds is hydrolyzed into sugar by amylase during the ripening process, and this provides a carbon source and energy for protein and oil synthesis (Marriott, Robinson, & Karikari, 1981). Interestingly, the starch content in the kernels under the two de-astringent treatments decreased and reached the lowest level on the 15th day, whereas the soluble sugar content, soluble protein, and oil content showed an upward trend and attained its highest value on the 15th day (Fig. 2), which was consistent with the results of our previous study (Zhang et al., 2020).

Different de-astringent treatments (ethanol, ethylene, CO_2, high temperature) may have different effects on the quality of the fruit. For example, a warm water treatment could remove astringency quickly. After short-term storage, the soluble sugar content increased, and this improved the taste and sensory quality of persimmons (Li, Wang, Lin, & Mao, 2020). Ethylene treatment promoted de-astringency and accelerated changes in the persimmon fruit texture and significantly promoted fruit softening after three days in storage (Min et al., 2012). The use an ionic solution of NaCl and alum combined with 1-MCP treatment to remove astringency can maintain the quality of persimmons well, and they exhibit reduced deterioration during storage. This result was primarily manifested as a better control of the change in color and hardness and a slowing down the loss of soluble sugar and ascorbic acid (Li et al., 2020). During the postharvest ripening process of *T. grandis*, the primary transformation of nutrients is the decomposition of starch to the synthesis of oil and protein (Zhang et al., 2020). In this study, Fig. 2 showed that there were no significant changes in the four primary nutrient compositions of *T. grandis* nuts under the $NaHCO_3$ treatment; that is, the $NaHCO_3$ treatment was an effective method for astringency removal without a significant effect on the nutritional quality of the *T. grandis* nuts. This result provides a valuable reference for research on the de-astringency of other nuts.

3.3. Overview analysis of the widely targeted metabolomics of *T. grandis* nuts processed with different de-astringent treatments

Metabolites are the basis of biological phenotypes and can help us effectively understand biological processes and mechanisms. Metabolomics, the qualitative and quantitative analysis of metabolites, can be used to detect, screen, and identify biologically significant metabolites in biological samples and to analyze metabolic pathways or networks (Zou et al., 2020). Based on the changes in the content of total phenols and soluble tannins under the postharvest de-astringent treatments, the study showed that their contents in the seed coat stabilized within 10 days, and those in the kernel stabilized within 15 days. Hence, we primarily analyzed the metabolite differences in the seed coat processed over 0–10 days and the kernel processed over 0–15 days.

A total of 293 metabolites were detected in the seed coats from 0 to 10 days, and the metabolites were mainly phenolic acids (92) and flavonoids (37) (Fig. S1A). In addition, a total of 347 metabolites were detected in the seed kernels from 0 to 15 days and the metabolites were also mainly concentrated in phenolic acids (101) and flavonoids (83) (Fig. S1B). Plant polyphenols, a class of important bioactive substances of plant origin, have antioxidant, anti-inflammatory, antitumor, lipid-lowering and cardiovascular-protecting activities and are important elements in the preparation of functional foods (Du et al., 2021). Some seed oils are also rich in phenolics, and these include tea seed oil (Liu et al., 2022) and sesame seed oil (Akpinar & Akca, 2021). In the principal component analysis (PCA) plot, the seed coat samples from the two de-astringent treatments revealed a distinct separation at both 5 and 10 days of ripening, suggesting that the seed coat at these two treatments had a relatively distinct metabolic profile (Fig. 3A). However, the kernel samples from the two de-astringent treatments were close in distance in the plot during the ripening time, indicating similarities in their metabolic profiles (Fig. 3C). We utilized a hierarchical cluster analysis to classify metabolites of the seed coat and kernel between the two treatments during ripening. The clustering results are displayed in a heatmap in Fig. 3B and Fig. 3D. In the heatmap, two highly distinct groups of differential metabolites of the seed coat in the CK and $NaHCO_3$ treatments were observed after 5 and 10 days of ripening time (Fig. 3B), and more differential metabolites in the seed coat were detected on Day 5 than on Day 10 of ripening. No distinct groups of differential metabolites were present in the kernels on Day 5 of ripening (Fig. 3D). Therefore, these results suggested that the metabolic profiles of the seed coat and kernel were different, especially on Day 5 of ripening.

3.4. Determination of the primary metabolites influenced by the different de-astringent treatments

To further determine the primary metabolites influenced by the $NaHCO_3$ treatments, we comparatively analyzed the differences in the metabolites of the CK and $NaHCO_3$ treatments on the 5th day. From 0 to 5 days, there were 120 and 140 different metabolites in the seed coats after the CK and $NaHCO_3$ treatments, respectively (Fig. S2A). There were 67 and 76 different metabolites in the kernels that underwent the CK and $NaHCO_3$ treatments, respectively (Fig. S2B). In addition, there were 34 common metabolites in the seed coats (Fig. 4A) and 11 common metabolites in the kernels (Fig. 4C). In addition, flavonoids, phenols, and tannins could be distinguished on the 5th day (Fig. 4B, 4D).

Both hydrolyzable and condensed tannins have the ability to interact with proteins and precipitate them, producing the tactile sensation of astringency (Xie & Dixon, 2005). By comparatively analyzing the changes in the key metabolites of the seed coats, the hydrolyzed tannins (gallic acid) did not significantly increase under the $NaHCO_3$ treatment, and there was no significant difference compared with the control nuts (Fig. S3A). Regardless of the different treatments, the content of the condensed tannins increased significantly from Day 0 to Day 5 (Fig. 1E and 1H). In a further comparison of the CK- and $NaHCO_3$-treated nuts on the 5th day, the contents of condensed tannins, including epigallocatechin, gallocatechin, procyanidin B1, procyanidin B2, procyanidin B3, and procyanidin C1, were markedly lower in the samples treated with the $NaHCO_3$ treatment (Table 2; Fig. S3; Table S1). The same analysis in the kernels indicated that the primary astringent substances were catechin, gallocatechin, and procyanidin B3 (Table 2; Fig. S3B; Table S1).

Currently, research on the astringent substance composition is primarily concentrated in tea, persimmons, and other plants. The astringent substance compositions of different plants are different. For example, the astringency in green tea is highly related to the concentration of epicatechin gallate (Ahmad, Gupta, & Mukhtar, 2000). The substances responsible for the astringent sensation of persimmon tannins are catechins and gallic acid (Tamura, Tanabe, Itai, & Hasegawa, 1999). The primary astringent substances in peanut skin are A-type proanthocyanidins (Lou et al., 1999). It was found that tannins in walnut fruit are the primary astringent substances by utilizing a comparison of seven astringent indices of thirty-eight walnut resources (Yu et al., 2020). Taken together, based on the comparative analysis of the metabolite contents on Day 5, epigallocatechin, gallocatechin, catechin, procyanidin B1, procyanidin B2, procyanidin B3, and procyanidin C1 were shown to be the primary metabolites influenced by the $NaHCO_3$ treatment, indicating their potential role as major contributors to the astringency of *T. grandis* nuts (Table 2). By clarifying the primary metabolite changes during the de-astringency process, this study has laid a good foundation for future research on the mechanism of nut de-

astringency.

4. Conclusions

This study provided the first comprehensive profile of the tentatively identified primary metabolites in *T. grandis* nuts during the postharvest de-astringent process. Our data showed that the $NaHCO_3$ treatment greatly reduced the contents of the total phenols and the soluble tannins and promoted the production of insoluble tannins and acetaldehyde. In addition, $NaHCO_3$ treatment did not affect the conversion of nutrients of *T. grandis* nuts after harvest, manifesting an effective way to remove the nut astringency. Moreover, the widely targeted metabolome analysis showed that the reduction of epigallocatechin, gallocatechin, catechin, procyanidin B1, procyanidin B2, procyanidin B3, and procyanidin C1 were significantly larger under the $NaHCO_3$ treatment compared with the CK treatment, revealing their potential roles in the astringency composition of *T. grandis* nuts. The research results provide new insights that will help guide further nut de-astringent research and provide a better understanding of quality improvement of the *T. grandis* nut.

CRediT authorship contribution statement

Lili Song: Conceptualization, Investigation, Writing – review & editing. **Xuecheng Meng:** Methodology, Investigation, Formal analysis, Validation. **Hanbing Song:** Formal analysis, Investigation, Validation. **Lingling Gao:** Methodology, Validation. **Yadi Gao:** Investigation, Formal analysis. **Wenchao Chen:** Investigation, Formal analysis. **Weiwei Huan:** Formal analysis. **Jinwei Suo:** Formal analysis. **Weiwu Yu:** Data curation. **Yuanyuan Hu:** Formal analysis, Data curation. **Baoru Yang:** Writing – review & editing. **Zuying Zhang:** Methodology, Investigation, Writing – original draft, Writing – review & editing. **Jiasheng Wu:** Conceptualization, Funding acquisition, Methodology, Supervision, Writing – review & editing.

Declaration of Competing Interest

The authors declare that they have no known competing financial interests or personal relationships that could have appeared to influence the work reported in this paper.

Data availability

Data will be made available on request.

Acknowledgments

This work was financially supported by the Key Research and Development Project of Zhejiang Province (2020C02019; 2021C02001; 2021C02013), the Zhejiang Provincial Academy Cooperative Forestry Science and Technology Project (2019SY07; 2021SY01), the National Natural Science Foundation of China (32101556; 31971699; 32001349), the Launching Funds for Zhejiang A&F University (2021FR019), the Zhejiang Provincial Science, Technology Innovation Activity for College Students (2020R412049), the Open Project Funds for State Key Laboratory of Subtropical Silviculture (KF201901), the Zhejiang Public Welfare Projects (LGN20C160002), the Zhejiang Provincial Natural Science Foundation of China (LQ19C160008), the Key Research Development Project of Zhejiang Province (2018C02004), the Selective Breeding of New Cultivars in T. grandis (2016C02052-12), and the 111 project (D18008). We thank LetPub (www.letpub.com) for their linguistic assistance during the preparation of this manuscript.

Appendix A. Supplementary data

Supplementary data to this article can be found online at https://doi.org/10.1016/j.foodchem.2022.133859.

References

Ahmad, N., Gupta, S., & Mukhtar, H. (2000). Green tea polyphenol epigallocatechin-3-gallate differentially modulates nuclear factor kB in cancer cells versus normal cells. *Archives of Biochemistry and Biophysics, 376*, 338–346. https://doi.org/10.1006/abbi.2000.1742

Akpinar, A., & Akca, S. (2021). The Effects of Grape, pomegranate, Sesame seed powder and their oils on probiotic ice cream: Total phenolic contents, antioxidant activity and probiotic viability. *Food Chemistry, 42*, Article 101203. https://doi.org/10.1016/j.fbio.2021.101203

Arnal, L., & Del Río, M. A. (2004). Effect of cold storage and removal astringency on quality of persimmon fruit (*Diospyros kaki*, L.) cv. Rojo Brillante. *Food Science and Technology International, 10*(3), 179–187. https://doi.org/10.1177/1082013204044824

Chazarra, S., Garcia-Carmona, F., & Cabanes, J. (2001). Hysteresis and positive cooperativity of iceberg lettuce polyphenol oxidase. *Biochemical Biophysical Research Communications, 289*(3), 769–775. https://doi.org/10.1006/bbrc.2001.6014

Chen, W., Gong, L., Guo, Z., Wang, W., Zhang, H., Liu, X., & Luo, J. (2013). A novel bintegrated method for large-scale detection, identification, and quantification of widely targeted metabolites: Application in the study of rice metabolomics. *Molecular Plant, 6*, 1769. https://doi.org/10.1093/mp/sst080

Cos, P., Bruyne, T. D., Hermans, N., Apers, S., Berghe, D. V., & Vlietinck, A. J. (2003). Proanthocyanidins in health care: Current and new trends. *Current Medicinal Chemistry, 11*(10), 1345–1359. https://doi.org/10.2174/0929867043365288

Dixon, R., Xie, D., & Sharma, S. (2005). Proanthocyanidins – a final frontier in flavonoid research? *New Phytologist, 165*, 9–28. https://doi.org/10.1111/j.1469-8137.2004.01217.x

Du, H., Wang, X., Yang, H., Zhu, F., Tang, D., Cheng, J., & Liu, X. (2021). Changes of phenolic profile and antioxidant activity during cold storage of functional flavored yogurt supplemented with mulberry pomace. *Food Chemistry, 132*, Article 108554. https://doi.org/10.1016/j.foodcont.2021.108554

Fan, S., Mu, H., Gao, H., Chen, H., Fang, X., & Wu, W. (2021). Study on alkaline deastringency of hickory kernel. *Acta Agriculturae Zhejiangensis, 33*(12), 2381–2389. in Chinese.

Gu, L., Kelm, M., Hammerstone, J., Beecher, G., Holden, J., Haytowitz, D., … Prior, R. (2004). Concentrations of proanthocyanidins in common foods and estimations of normal consumption. *The Journal of Nutrition, 134*(3), 613–617. https://doi.org/10.1093/jn/134.3.613

Han, C., Li, J., Jin, P., Li, X., Wang, L., & Zheng, Y. (2017). The effect of temperature on phenolic content in wounded carrots. *Food chemistry, 215*, 116–123. https://doi.org/10.1016/j.foodchem.2016.07.172

Haslam, E. (1977). Symmetry and promiscuity in procyanidin biochemistry. *Phytochemistry, 16*, 1625–1640. https://doi.org/10.1016/0031-9422(71)85060-4

He, M., Tian, H., Luo, X., Qi, X., & Chen, X. (2015). Molecular Progress in Research on Fruit Astringency. *Molecules, 20*, 1434–1451. https://doi.org/10.3390/molecules20011434

Hu, Y., Zhang, Z., Hua, B., Tao, L., Chen, W., Gao, Y., … Song, L. (2022). The interaction of temperature and relative humidity affects the main aromatic components in postharvest *Torreya grandis* nuts. *Food chemistry, 368*, Article 130836. https://doi.org/10.1016/j.foodchem.2021.130836

Huang, R., & Xu, C. M. (2020). An overview of the perception and mitigation of astringency associated with phenolic compounds. *Comprehensive Reviews in Food Science and Food Safety, 20*, 1036–1074. https://doi.org/10.1111/1541-4337.12679

Hu, H., Wang, J., Hu, Y., & Xie, J. (2020). Nutritional component changes in Xiangfen 1 banana at different developmental stages. *Food & Function, 11*(9), 8286–8296.

Li, H. M., Wang, Y. M., Lin, F., & Mao, R. F. (2020). Effects of de-astringent treatment combined with 1–MCP fresh preservation technology on storage quality of Gongcheng persimmon. *Journal of Light Industry, 35*(5), 16–25. in Chinese.

Liu, G. Y., Zhu, W. Q., Zhang, J., Song, D. D., Zhuang, L. W., Ma, Q., … Xu, X. (2022). Antioxidant capacity of phenolic compounds separated from tea seed oil in vitro and in vivo. *Food Chemistry, 371*, Article 131122. https://doi.org/10.1016/j.foodchem.2021.131122

Li, X., & Li, J. (2013). Determination of the Content of Soluble Sugar in Sweet Corn with Optimized Anthrone Colorimetric Method. *Storage and Process, 13*(04), 24–27. in Chinese.

Lou, H., Yamazaki, Y., Sasaki, T., Uchida, M., Tanaka, H., & Oka, S. (1999). A-type proanthocyanidins from peanut skins. *Phytochemistry, 51*, 297–308. https://doi.org/10.1016/S0031-9422(98)00736-5

Marriott, J., Robinson, M., & Karikari, S. (1981). Starch and sugar transformation during the ripening of plantains and bananas. *Journal of the Science of Food and Agriculture, 32*, 1021–1026. https://doi.org/10.1002/jsfa.2740321011

Min, T., Yin, X. R., Shi, Y. N., Luo, Z. R., Yao, Y. C., Grierson, D., … Chen, K. S. (2012). Ethylene-responsive transcription factors interact with promoters of *ADH* and *PDC* involved in persimmon (*Diospyros kaki*) fruit de-astringency. *Journal of Experimental Botany, 63*(18), 6393–6405. https://doi.org/10.1093/jxb/ers296

Oshida, M., Yonemori, K., & Sugiura, A. (1996). On the nature of coagulated tannins in astringent-type persimmon fruit after an artificial treatment of astringency removal. *Postharvest Biology Technology, 8*, 317–327. https://doi.org/10.1016/0925-5214(96)00016-6

Pesis, E. (2005). The role of the anaerobic metabolites, acetaldehyde and ethanol, in fruit ripening, enhancement of fruit quality and fruit deterioration. *Postharvest Biology Technology, 37*, 1–19. https://doi.org/10.1016/j.postharvbio.2005.03.001

Read, S., & Northcote, D. (1981). Minimization of variation in the response to different protein of the Coomassic Blue G dye binding assay for protein. *Analytical Biochemistry, 116*, 53–64. https://doi.org/10.1016/0003-2697(81)90321-3

Serrano, J., Puupponen-Pimiä, R., Dauer, A., Aura, A. M., & Saura-Calixto, F. (2009). Tannins: Current knowledge of food sources, intake, bioavailability and biological effects. *Molecular Nutrition & Food Research, 53*, S310–S329. https://doi.org/10.1002/mnfr.200900039

Soares, S., Brandão, E., Guerreiro, C., Soares, S., Mateus, N., & Freitas, V. D. (2020). Tannins in food: Insights into the molecular perception of astringency and bitter taste. *Molecules, 25*, 2590. https://doi.org/10.3390/molecules25112590

Suo, J., Tong, K., Wu, J., Ding, M., Chen, W., Yang, Y., … Song, L. (2019). Comparative transcriptome analysis reveals key genes in the regulation of squalene and β-sitosterol biosynthesis in *Torreya grandis*. *Industrial Crops and Products, 131*, 182–193. https://doi.org/10.1016/j.indcrop.2019.01.035

Tamura, F., Tanabe, K., Itai, A., & Hasegawa, M. (1999). Characteristics of acetaldehyde accumulation and removal of astringency with ethanol and carbon dioxide treatment in "Saijo" persimmon. *Journal of the Japanese Society for Horticultural Science, 68*(6), 1178–1183. http://en.cnki.com.cn/Article_en/CJFDTotal-BZGC201919004.htm.

Taira, S., Ikeda, K., & Ohkawa, K. (2001). Comparison of insolubility of tannins induced by acetaldehyde vapor in fruit of three types of astringent persimmon. *Journal of the Japanese Society for Horticultural Science, 48*, 684–687.

Wei, X., Ju, Y., Ma, T., Zhang, J., Fang, Y., & Sun, X. (2020). New perspectives on the biosynthesis, transportation, astringency perception and detection methods of grape proanthocyanidins. *Critical Reviews in Food Science and Nutrition, 61*(14), 2372–2398. https://doi.org/10.1080/10408398.2020.1777527

Xie, D. Y., & Dixon, R. A. (2005). Proanthocyanidin biosynthesis–still more questions than answers? *Phytochemistry, 66*, 2127–2144. https://doi.org/10.1016/j.phytochem.2005.01.008

Xu, Y., Zhang, Y., Chen, J., Wang, F., Du, Q., & Yin, J. (2018). Quantitative analyses of the bitterness and astringency of catechins from green tea. *Food chemistry, 258*, 16–24. https://doi.org/10.1016/j.foodchem.2018.03.042

Yang, M., Yang, J., Su, L., Sun, K., Li, D., Liu, Y., … Guo, T. (2019). Metabolic profile analysis and identification of key metabolites during rice seed germination under low-temperature stress. *Plant Science, 289*, Article 110282. https://doi.org/10.1016/j.plantsci.2019.110282

Yin, X. R., Shi, Y. N., Min, T., Luo, Z. R., Yao, Y. C., Xu, Q., … Chen, K. S. (2012). Expression of ethylene response genes during persimmon fruit astringency removal. *Planta, 235*, 895–906. https://www.jstor.org/stable/43564723.

Yu, W., Jin, Q., Li, G., Zhang, R., Wu, C., Wang, X., & Yu, J. (2020). Analysis of the genetic diversity of Xinjiang walnut resources based on the bitterness of the fruit. *Food Industry Science and Technology, 41*(13), 234–240. in Chinese.

Zhang, W., Li, X., Zheng, J., Wang, G., Sun, C., Ferguson, I. B., & Chen, K. (2008). Bioactive components and antioxidant capacity of Chinese bayberry (*Myrica rubra* Sieb. and Zucc.) fruit in relation to fruit maturity and postharvest storage. *European Food Research and Technology, 227*, 1091–1097.

Zhang, Z., Jin, H., Suo, J., Yu, W., Zhou, M., Dai, W., Song, L., Hu, Y., & Wu, J. (2020). Effect of temperature and humidity on oil quality of harvested *Torreya grandis* cv. Merrillii Nuts during the after-ripening stage. *Frontiers in Plant Science*. https://doi.org/10.3389/fpls.2020.573681. doi: 10.3389/fpls.2020.573681

Zhou, M., Song, L., Ye, S., Zeng, W., Hännien, H., Yu, W., … Wu, J. (2019). New sights into lipid metabolism regulation by low temperature in harvested *Torreya grandis* nuts. *Journal of the Science of Food and Agriculture., 99*, 4226–4234. https://doi.org/10.1002/jsfa.9653

Zou, S., Wu, J., Shahida, M., He, Y., Lin, S., Liu, Z., & Yang, X. (2020). Identification of key taste components in loquat using widely targeted metabolomics. *Food chemistry, 323*, Article 126822. https://doi.org/10.1016/j.foodchem.2020.126822